Improving Microcirculatory Reperfusion Reduces Parenchymal Oxygen Radical Formation and Provides Neuroprotection

Aslihan Taskiran-Sag, MD; Muge Yemisci, MD, PhD; Yasemin Gursoy-Ozdemir, MD, PhD; Sefik Evren Erdener, MD, PhD; Hulya Karatas, MD, PhD; Deniz Yuce, MD; Turgay Dalkara, MD, PhD

Background and Purpose—Reperfusion is the most significant determinant of good outcome after ischemic stroke. However, complete reperfusion often cannot be achieved, despite satisfactory recanalization. We hypothesized that microvascular protection was essential for achieving effective reperfusion and, hence, neuroprotection. To test this hypothesis, we have developed an in vivo model to differentially monitor parenchymal and vascular reactive oxygen species (ROS) formation. By comparing the ROS-suppressing effect of N-tert-butyl-α-phenylnitrone (PBN) with its blood–brain barrier impermeable analog 2-sulfo-phenyl-N-tert-butylnitrone (S-PBN), we assessed the impact of vascular ROS suppression alone on reperfusion and stroke outcome after recanalization.

Methods—The distal middle cerebral artery was occluded for 1 hour by compressing with a micropipette and then recanalized (n=60 Swiss mice). ROS formation was monitored for 1 hour after recanalization by intravital fluorescence microscopy in pial vasculature and cortical parenchyma with topically applied hydroethidine through a cranial window. PBN (100 mg/kg) or S-PBN (156 mg/kg) was administered shortly before recanalization, and suppression of the vascular and parenchymal hydroethidine fluorescence was examined (n=22). Microcirculatory patency, reperfusion, ischemic tissue size, and neurological outcome were also assessed in a separate group of mice 1 to 72 hours after recanalization (n=30).

Results—PBN and S-PBN completely suppressed the reperfusion-induced increase in ROS signal within vasculature. PBN readily suppressed ROS produced in parenchyma by 88%. S-PBN also suppressed the parenchymal ROS by 64% but starting 40 minutes later. Intriguingly, PBN and S-PBN comparably reduced the size of ischemic area by 65% and 48% ($P>0.05$), respectively. S-PBN restored the microvascular patency and perfusion after recanalization, suggesting that its delayed parenchymal antioxidant effect could be secondary to improved microcirculatory reperfusion.

Conclusions—Promoting microvascular reperfusion by protecting vasculature can secondarily reduce parenchymal ROS formation and provide neuroprotection. The model presented can be used to directly assess pharmacological end points postulated in brain parenchyma and vasculature in vivo.

Visual Overview—An online visual overview is available for this article. **(*Stroke*. 2018;49:1267-1275. DOI: 10.1161/STROKEAHA.118.020711.)**

Key Words: animals ■ ischemia ■ neuroprotection ■ nitrones ■ no-reflow phenomenon ■ reactive oxygen species ■ reperfusion injury

Despite large body of experimental data showing successful use of neuroprotective agents in acute ischemic stroke treatment, translation of these findings to clinic has not been promising, suggesting that there is still much remaining to be learned.[1–3] One of the outstanding issues is that majority of animal neuroprotection studies did not specifically examine patency of the microvasculature, which is essential for satisfactory reperfusion after recanalization and, hence, to achieve parenchymal protection.[4,5] The latter idea may seem to be obvious because recanalization in humans and experimental animals can rescue the penumbral tissue without any supplementary neuroprotective therapy. However, recent clinical trials consistently show that despite successful recanalization, reperfusion of the ischemic tissue is often incomplete and that a

Received September 5, 2017; final revision received March 17, 2018; accepted March 20, 2018.

From the Institute of Neurological Sciences and Psychiatry (A.T.-S., M.Y., Y.G.-O., S.E.E., H.K., T.D.), Department of Neurology (M.Y., Y.G.-O., T.D.), and Institute of Cancer (D.Y.), Hacettepe University, Ankara, Turkey.

Current address for Dr Gursoy-Ozdemir: Department of Neurology, Koc University, İstanbul, Turkey.

Current address for Dr Erdener: Optics Division, Athinoula A. Martinos Center for Biomedical Imaging, Massachusetts General Hospital, Harvard Medical School, Charlestown.

Presented in part at the Society for Neuroscience 46th Annual Meeting, Neuroscience 2016, San Diego, CA, November 12–16, 2016.

The online-only Data Supplement is available with this article at http://stroke.ahajournals.org/lookup/suppl/doi:10.1161/STROKEAHA.118.020711/-/DC1.

Correspondence to Turgay Dalkara, MD, PhD, Institute of Neurological Sciences and Psychiatry, Hacettepe University, Ankara, Turkey. E-mail tdalkara@hacettepe.edu.tr

favorable outcome is best correlated with satisfactory reperfusion.[6] These observations suggest that success of recanalization therapies can be improved by diminishing incomplete reperfusion (no-reflow) caused by loss of patency of some microvessels during ischemia that persists after recanalization.[5,7]

Supporting the above view, a low dose of blood–brain barrier (BBB)-impermeable NO synthase inhibitor (L-N^5-[1-iminoethyl]-ornithine) was equally neuroprotective to its BBB-permeable analog (low-dose N^{ω}-nitro-L-arginine) when given 2 hours after middle cerebral artery occlusion (MCAo).[8] L-N^5-(1-iminoethyl)-ornithine, which is unlikely to pass through the BBB because the paracellular pathway is still closed to polar molecules at this early time point of ischemia, was shown to improve microcirculatory reperfusion after recanalization. A subsequent study that specifically investigated BBB penetration of H^3-labeled adenosine after 2-hours of MCAo reported a striking neuroprotection with adenosine nanoparticles, despite the finding that adenosine did not penetrate into the parenchyma, supporting the idea that by improving reperfusion alone, it was possible to obtain neuroprotection.[9] In fact, the potential significance of microcirculatory reflow after stroke has been subject of many studies for the past 50 years.[7,10] For example, a similar observation to the above was made with N-tert-butyl-α-phenylnitrone (PBN) and its derivatives long time ago; 2-sulfo-phenyl-N-tert-butylnitrone (S-PBN), which is BBB impermeable, was found to be equally neuroprotective to PBN that is highly liposoluble.[11] However, the patency of microvasculature, its correlation with the neuroprotection observed, and antioxidant effect of S-PBN were not studied in the latter study as in many other past studies. Based on this gap in the literature, a commentary by a group of stroke researchers in the aftermath of SAINT-II trial (Stroke–Acute Ischemic NXY Treatment-II) rightly recommended that the assumptions on the antioxidant actions of drugs must be directly assessed in stroke models at both pharmacodynamic and pharmacokinetic levels.[12]

In line with these recommendations, we monitored reactive oxygen species (ROS) formation during ischemia/recanalization (i/r) on the vascular wall and in parenchymal cells in a mouse MCAo model by using intravital fluorescence imaging and then differentially studied the effects of PBN and S-PBN on extinguishing ROS in both compartments. This approach clearly documented that PBNs at the doses used suppressed ROS formation during recanalization. By taking advantage of S-PBN being BBB impermeable, we have been able to show that inhibiting ROS toxicity solely in the vasculature during recanalization can provide neuroprotection by promoting microvascular reperfusion. Therefore, diminishing no-reflow seems to be an important and viable target for recanalization therapies, and the model developed can be used to optimize the antioxidant treatments for improving their translational potential.

Materials and Methods

A detailed Methods section can be found in the online-only Data Supplement. We declare that all data and the supporting materials are available within the article and its online-only Data Supplement.

Focal Ischemia/Recanalization

Male Swiss mice weighing 31±1 g were anesthetized with urethane (750 mg/kg intraperitoneally [IP] for induction followed by 500 mg/kg supplement 30 minutes later). Urethane has almost no effect on cerebral blood flow (CBF), making it advantageous for ischemia research. Animals breathed a mixture of room air and supplemental oxygen through a face mask for the duration of the experiment, and the O_2 flow rate was varied (around 2 L/min) to maintain tissue O_2 saturation above 92% to avoid anesthesia-induced hypoxia. Oxygen saturation, pulse rate, and body temperature were monitored and maintained within the physiological range. Animal housing, care, and the experimental procedures were all done in accordance with institutional guidelines. The study was approved by Hacettepe University Ethics Committee (2010–21/5 and 2018/07-02).

We occluded distal main trunk of the right middle cerebral artery (MCA) by compressing with a blunted glass micropipette (50–70 µm tip) as described previously[13] (Figure 1A). Recanalization was obtained by retracting the micropipette. Ischemia (1 hour) and recanalization (1 hour) were confirmed by recording regional cerebral blood flow (rCBF) with laser speckle contrast imaging.[14] The details of the rCBF measurements can be found in the online-only Data Supplement.

Intravital Imaging of ROS

We opened a 2×2-mm cranial window, leaving the dura intact and filled with artificial cerebrospinal fluid at 37°C to maintain cortical physiological conditions. We added hydroethidine (Molecular Probes, 16 µM in 0.1% DMSO) into artificial cerebrospinal fluid 5 minutes before recanalization to monitor ROS formation by intravital fluorescent imaging under a stereomicroscope (Nikon SMZ1000) in a dark room. After recanalization, hydroethidine was washed out, and the cranial window was refilled with artificial cerebrospinal fluid. Fluorescent images of pial arterioles of 25 to 40 µm in diameter and venules of 30 to 60 µm together with cortical surface were captured every 2 minutes for the first half an hour and then every 5 minutes for another half an hour after recanalization (excitation, 543 nm; emission, >570 nm; exposure duration, 1.5 seconds) by using a CCD camera (Nikon DS-Qi1Mc) and NIS Elements Advanced Research Software v3.2.

Although hydroethidine can be oxidized by some other radical species too, limiting its use for quantifying superoxide formation,[15] this well-characterized fluoroprobe can still be used in vivo to semiquantitatively (eg, relative changes from baseline) monitor oxygen radical scavenging by nitrones.

Experimental Groups

A total of 63 mice were used for this study, 3 of which were sham operated.

Twenty-two mice were used for imaging ROS formation with hydroethidine. These mice were IP injected with either saline (n=6), PBN (n=7), or S-PBN (n=6) or were sham operated (n=3). Mice were allocated to groups by simple randomization; treatment compounds were applied in a randomized fashion, and the researcher who performed the in vivo experiments was blinded toward the treatment each mouse received. After 1 hour ischemia and 1 hour recanalization (1 hour i/r), mice were euthanized under high-dose chloral hydrate (1000 mg/kg, IP). To assess the effect of PBN and S-PBN on ischemia outcome (neuroprotection) and microcirculatory no-reflow, we used another set of mice that were injected with either saline (n=6), PBN (n=6) or S-PBN (n=6). These mice were euthanized 1 hour after recanalization.

PBN (100 mg/kg, IP) was administered 15 minutes before recanalization. S-PBN (156 mg/kg, IP) was administered twice, 10 minutes and just before recanalization. S-PBN was given twice because of its shorter half-life (9 minutes)[16] compared with PBN (3 hours).[17]

Image Analysis

We used ImageJ 1.48v and NIS Elements AR v3.2 software for analyzing fluorescent signal changes in vivo. The analyst was blind to the treatment. We carefully placed 10 regions of interest (ROIs) under high magnification using point-selection tool of ImageJ that can select pixel-sized ROIs on arteriolar and venular walls and exclude perivascular signals. The relative changes in signal intensity from baseline (not the absolute values) were measured during the course of recanalization.

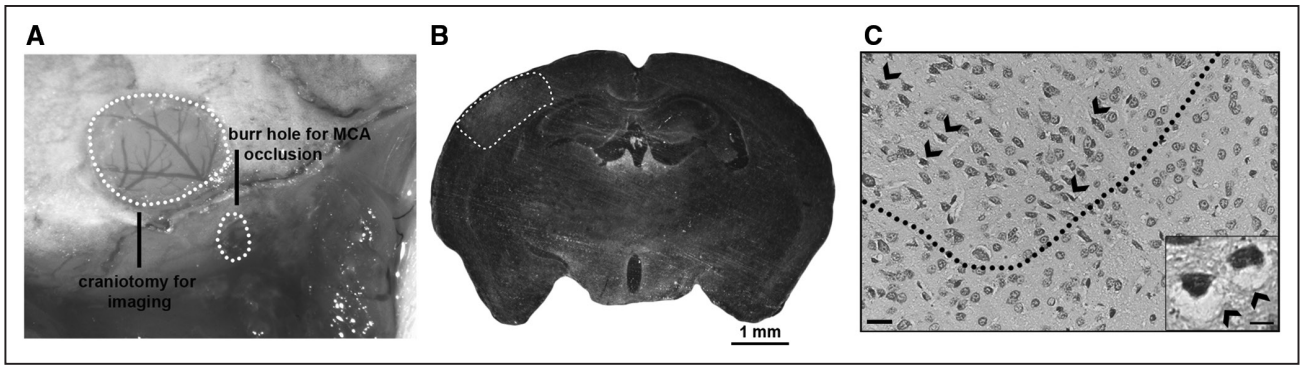

Figure 1. Experimental setup and the ischemic changes induced by transient distal middle cerebral artery (MCA) occlusion. For imaging of cortex and pial vessels, a 2×2-mm cranial window was prepared after parietal craniotomy. Distal main trunk of the right MCA was exposed through a burr hole in the temporal bone 2 mm superior to the zygomatic arch and occluded by compressing with a blunted glass micropipette. Dura was kept intact (**A**). After 1 hour ischemia and 1 hour recanalization, ischemic tissue (encircled by the white dashed line) was visible by changes in tissue transmittance of Nissl-stained sections with phase-contrast microscopy (**B**). The ischemic MCA area (above the black dashed line) exhibited cellular edema and nuclear condensation at this early time point during the course of infarct development. Inset shows an image of 2 shrunken parenchymal cells exhibiting nuclear condensation and pericellular swelling. Arrowheads depict ischemic cells (**C**; scale bar in [**C**]=20 μm; in inset, 5 μm).

Measurement of the parenchyma signal intensity was complicated by lack of a sharp boundary delineating the cell from the surrounding neuropil. Accordingly, cellular signals within parenchymal ROIs of 0.01 mm^2 were semiquantitatively graded as weak, moderate, strong, and very strong according to their intensity. The same vascular and parenchymal ROIs were tracked throughout 1-hour recanalization.

Assessment of Neuroprotection, Microcirculatory No-Reflow, and BBB Integrity

Mice (n=18) were transcardially perfused with heparin (1000 IU/100 mL saline) followed by 4% paraformaldehyde (in phosphate-buffered saline) to thoroughly flush vessels out of blood. Brains were removed and kept in 4% paraformaldehyde for 24 hours. Five micrometer thick coronal sections were prepared from paraffin-embedded tissues and stained with cresyl violet. The ischemic area on coronal brain sections passing through the middle of cranial window where ROS measurements were obtained was delineated on Nissl-stained sections under phase-contrast microscope and measured on images captured by using NIS Elements AR v4.2 software (Figure 1B).

To assess the magnitude of no-reflow, paraffin-embedded sections were treated with 0.2% sodium borohydride in phosphate-buffered saline to render erythrocytes visible by reducing hemoglobin, hence, making it fluorescent.[8,18] Microvascular segments with entrapped erythrocytes were counted in the ischemic cortex. To study the BBB integrity, 3 additional mice were transcardially perfused at the end of 1-hour i/r. Evans blue was injected IP on the 30th minute of recanalization (4% in saline, 200 μL) and repeated during transcardial perfusion. The brains were removed, and 20-μm-thick cryosections were analyzed under confocal microscope (Leica TCS SP8 DLS; Wetzlar, Germany).

The corner turn and adhesive removal tests were performed by 2 independent researchers to assess functional outcome in another group of S-PBN–treated and saline-treated mice after 1-hour i/r (n=6 per group). The mice were tested before surgery, 6, 24, 48, and 72 hours after transient MCAo.

Statistics

The values were presented as means with their SEM. Repeated measures designs in linear models were used for analyses to compare temporal changes of dependent variables. P values <0.05 were considered as statistically significant. Kruskal–Wallis and Mann–Whitney U tests were used to compare the parenchymal fluorescence intensity counts, ischemic area size, CBF changes, number of microvascular segments with entrapped red blood cells, and behavioral test results. Analyses were performed with SPSS21 (IBM Corp, Armonk, NY) and supervised by a statistician (D.Y.).

Results

The physiological parameters of the 63 mice studied were within the normal range (tissue oxygen saturation, 93%–100%; pulse rate, 380–450 per minute; temperature, 36.8–37.0°C).

Distal MCA Ischemia

In fluorescent imaging experiments, the rCBF within 4 ROIs in the penumbral MCA territory under the cranial window was 45.9±1.6% (mean±SEM of 19 mice in 3 groups) in agreement with the original report describing the model,[13] as well as the penumbral values detected by laser speckle contrast imaging after ligation of the distal MCA.[19,20] Possibly because laser speckle contrast imaging is more sensitive to rCBF changes at the cortical surface and also to lateral scattering from pial vessels, the penumbral ischemic flow values detected were relatively higher than measured by other methods.[21] There was not any significant difference in the level of ischemia attained between the 3 experimental groups, in which ROS generation was monitored (saline, 43.8±2.7%; PBN, 47.3±2.6%; S-PBN, 46.5±3.6%).

ROS Production in Vascular Wall

Recanalization of the MCA after 1-hour ischemia resulted in a robust increase in ROS production both on pial arteriolar and venular walls (Figure 2A through 2C). The fluorescent signal measured with the ROIs placed over the arteriolar wall increased to 176±24% of the basal intensity within the first 30 minutes of the recanalization and remained >160% throughout the second half hour (Figure 2B and 2C). Both PBN (100 mg/kg) and S-PBN (156 mg/kg; equimolar to PBN 100 mg/kg) administered shortly before recanalization completely suppressed the increase in ROS signal starting from the beginning of the recanalization (P<0.001).

Although there are other potential targets of PBN than ROS,[22–24] suppression of the hydroethidine fluorescence by nitrones strongly suggests that the signal originated from ROS. This was further confirmed by showing that inhibition of NADPH oxidase—a major source of ROS—during i/r by apocynin (2.5 mg/kg, IP, 30 minutes before recanalization;

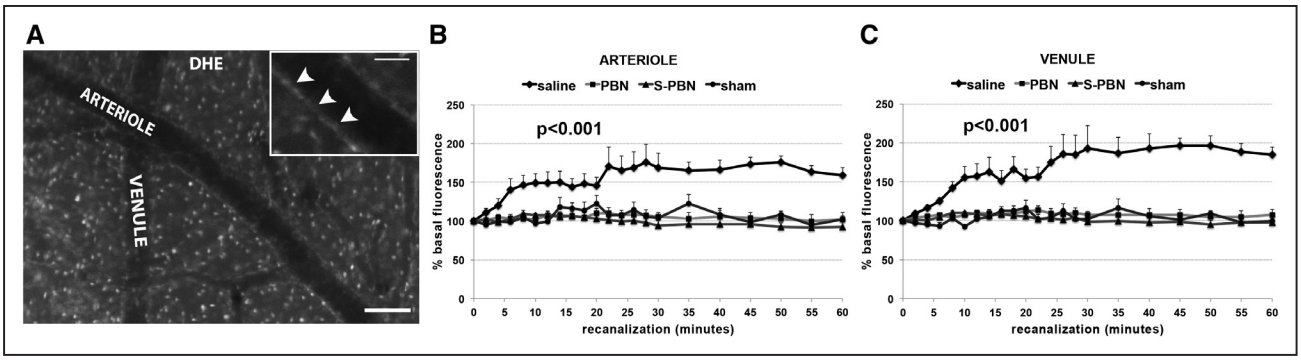

Figure 2. Recanalization induced reactive oxygen species (ROS) formation on cortical pial vessels. ROS formation was detected by hydroethidine (DHE) fluorescence (**A**). The image was captured on the 30th min of recanalization after 1 hour ischemia. Inset shows arteriole at higher magnification; arrowheads point to the vascular wall strip where the DHE signal was measured. Because the images were acquired by capturing emission for 1.5 s, the rapidly circulating blood cells did not contribute to the static images displayed. DHE fluorescence arising on the vascular wall showed a robust increase during 1-hour recanalization after 1-hour middle cerebral artery (MCA) ischemia compared with prerecanalization levels (**B** and **C**). N-tert-butyl-α-phenylnitrone (PBN; n=7) and 2-sulfo-phenyl-N-tert-butylnitrone (S-PBN; n=6) administered shortly before recanalization significantly suppressed the ROS signal down to values measured in sham-operated mice (no MCA occlusion) starting from the beginning of recanalization (**B** and **C**; $P<0.001$ vs saline-treated group; scale bar in [**A**]=50 μm; in inset, 20 μm).

n=6) strongly suppressed pial arteriolar and venular ROS signals (Figure I in the online-only Data Supplement).

ROS Production in Parenchyma

Unlike the vascular wall where the fluorescent signal formed a continuous narrow band along the vessel wall, the parenchymal signal appeared as spheres of 8 to 10 μm. Nuclear labeling with YOYO-1 applied into the cranial window (8 μmol/L for 5 minutes; n=2) showed that these fluorescent spheres corresponded to parenchymal cells. Removing the dura did not modify distribution of the spherical signals ensuring that dural cells (mostly spindle-shaped fibroblasts with 15–25-μm nuclear size) did not contribute to these signals.

Majority of the parenchymal cells exhibited strong/very strong fluorescence starting 10 minutes after recanalization in saline-injected controls (Figure 3). PBN significantly suppressed the ROS signal from the beginning of recanalization such that only weak and moderate signals were observed ($P<0.05$ versus saline-treated group). The intensity of remaining signals was within the same range with the ROS signal observed in sham-operated mice. On the other hand, the suppressive effect of S-PBN was partial and delayed (by 64% 1 hour after recanalization) and was found to be significantly different from the saline-treated mice values only toward the end of the monitoring starting on the 40th minute ($P=0.03$; Figure 3).

Neuroprotection

In neuroprotection experiments, the decrease in rCBF within 4 ROIs in the penumbral MCA territory was 42.6±1.8% (n=18 mice in 3 groups). The level of ischemia was not significantly different between the groups (Table). Occlusion of the distal MCA for 1 hour with this method had previously been shown to cause pannecrosis involving the cortex fed by the distal MCA when detected 72 hours after ischemia.[13] However, to be able to correlate the microcirculatory dysfunction and intensity of ischemic injury with the antioxidant action of PBN and S-PBN observed above, we examined the histological changes after 1-hour i/r because pathological cascades that will take place later can confound subsequent histological changes. We took liberty to take this approach because PBNs were repeatedly shown to reduce the infarct volume detected at 24 hours after MCAo in rodents.[22–25] At this early time point during the course of infarct development, the ischemic MCA area exhibited cellular edema and nuclear condensation (Figure 1C). We were able to delineate this area by changes in tissue transmittance of Nissl-stained sections with phase-contrast microscopy (Figure 1B). We found that 1-hour i/r in saline-treated controls resulted in an ischemic zone of 1557±313 μm^2 in the ipsilateral cortex under the cranial window where ROS measurements were obtained. PBN and S-PBN both significantly reduced the ischemic area (552±116 μm^2, $P=0.01$; 807±71 μm^2, $P=0.03$, respectively; Figure 4B), suggesting that despite the fact that S-PBN has direct effect only on the vascular wall as demonstrated above (Figures 2 and 3), it can provide similar degree of neuroprotection to PBN ($P=0.15$ versus S-PBN–treated group; Figure 4B). To assess whether or not this neuroprotection is sustainable, we evaluated the sensorimotor function (the main neurological deficit developing in distal MCA occlusion models[26,27]), 6, 24, 48, and 72 hours after 1-hour i/r. S-PBN–treated mice had significantly better outcome with corner turn and adhesive tape removal tests compared with saline-treated mice (n=6 mice per group; Figure 4C and 4D).

Microcirculatory No-Reflow

The robust and rapid suppression of vascular ROS signal by S-PBN followed by a delayed parenchymal antioxidant effect led to the hypothesis that its parenchymal effect could be secondary to improvement of the microcirculatory reflow because S-PBN is a highly polar, BBB-impermeable molecule; hence, it is not expected to penetrate parenchyma at this early time point after ischemia.[28] To assess this possibility, we first confirmed that the BBB was intact at the end of 1-hour i/r by showing that systemically administered Evans blue did not leak into tissue (n=3; Figure 5A). We then quantified the capillary segments with entrapped erythrocytes (indicating microcirculatory no-reflow),[8] after 1-hour i/r. This analysis revealed that S-PBN indeed significantly restored the

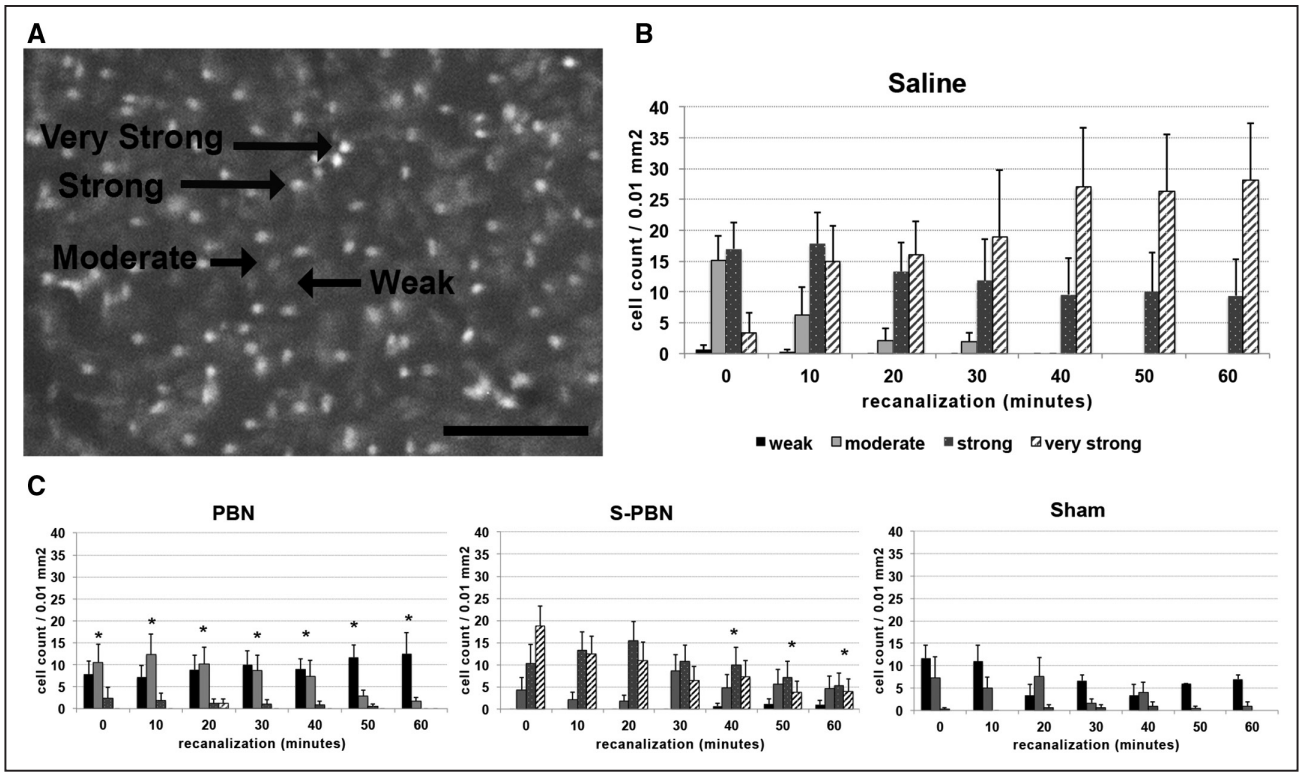

Figure 3. Recanalization induced reactive oxygen species (ROS) formation in parenchyma. Parenchymal cells exhibited strong/very strong hydroethidine fluorescence after recanalization in saline-treated control mice (**A**). N-tert-butyl-α-phenylnitrone (PBN) significantly reduced the reperfusion-induced ROS increase to the values comparable with the sham-operated (no occlusion) mice starting from the beginning of recanalization (**B** and **C**). The ROS-suppressing effect of 2-sulfo-phenyl-N-tert-butylnitrone (S-PBN) on parenchymal cells was partial and delayed and was found to be significantly different from the saline-treated mice values starting on the 40th min. *P<0.05 compared with saline-treated group (scale bar=50 μm).

microvascular patency (saline, 158±24 microvessel segments per mm^2; S-PBN, 105±18 microvessel segments per mm^2, P=0.05 versus saline; PBN, 72±22 microvessel segments per mm^2, P=0.04 versus saline; n=6 per group; Figure 4A and 4B).

Regional CBF Change After Recanalization

To verify that S-PBN might have improved microcirculation after recanalization, we calculated the mean rCBF change within 4 ROIs throughout 1-hour recanalization recorded with laser speckle contrast imaging, which basically monitors the microcirculatory flow. Despite the comparable levels of ischemia in all groups, postrecanalization measurements obtained from the same 4 ROIs in the ischemic area revealed that the mean rCBF recovery was not complete within 1 hour after recanalization in the saline-treated group (values are given in the Table). In contrast, S-PBN and PBN completely restored tissue reperfusion after recanalization (P<0.05 versus saline-treated group; Table; Figure 5B).

Table. Average rCBF Change During Ischemia and Recanalization

	Ischemia	Recanalization
	ΔCBF, %*	ΔCBF, %*
Saline (n=6)	−40.9±2.8	−14.3±1.8
S-PBN (n=6)	−42.8±2.5	6.2±3.7 (P=0.004 vs saline)
PBN (n=6)	−44.1±4.3	2.8±4.4 (P=0.01 vs saline)
	P=0.63	P=0.006

P values were calculated using Kruskal–Wallis test, and Mann–Whitney U test was used for further comparisons. CBF indicates cerebral blood flow; i/r, ischemia/recanalization; PBN, N-tert-butyl-α-phenylnitrone; and S-PBN, 2-sulfo-phenyl-N-tert-butylnitrone.

*Values are the average changes in CBF compared with baseline (mean±SEM) during 1 h i/r.

Discussion

Our findings demonstrate that PBN can suppress parenchymal and vascular wall oxygen radical generation during reperfusion, whereas its BBB-impermeable derivative, S-PBN, has direct effect only on vascular wall as anticipated.[22,23,29] However, both agents provided similar degree of neuroprotection, and detailed studies showed that S-PBN secondarily decreased parenchymal oxygen radical generation by improving microcirculatory reflow after recanalization. These findings illustrate, to our knowledge for the first time, that promoting reperfusion by microvascular protection can indirectly reduce parenchymal radical toxicity and provide neuroprotection.

Although neuroprotective action of radical scavengers is a much investigated subject, their effects have rarely been studied at cellular level in vivo by differentiating the parenchymal and vascular compartments.[30] Our model allowed us to simultaneously achieve these goals under in vivo conditions. With this approach, we were able to directly assess the targeted pharmacological end points in situ at cellular level

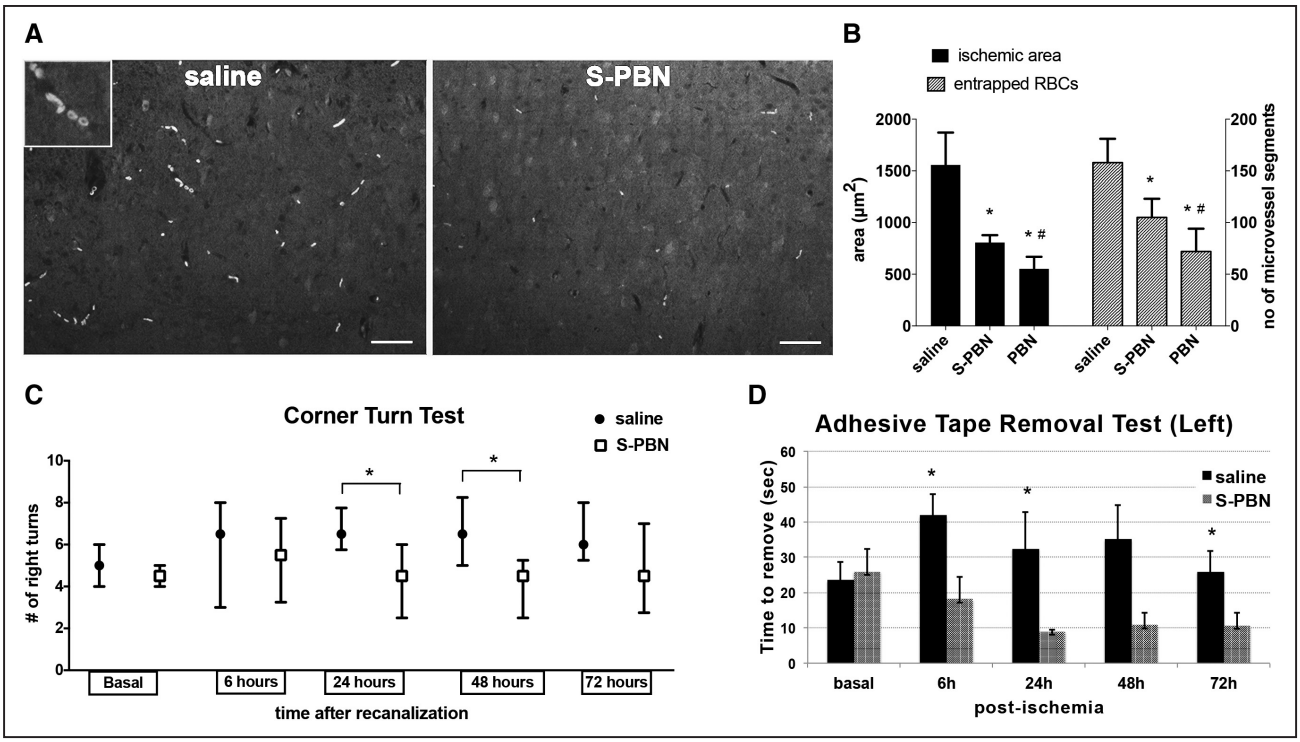

Figure 4. Microcirculatory no-reflow and neurological function are restored by 2-sulfo-phenyl-N-tert-butylnitrone (S-PBN). **A**, Entrapped red blood cells (RBCs) within microvessel segments in the cortex of a saline-injected mouse (**left**) and an S-PBN–injected mouse (**right**) after 1 hour ischemia and 1 hour recanalization. Brain sections were incubated with sodium borohydride to render erythrocytes fluorescent. Inset shows magnified view of entrapped erythrocytes in a microvessel. S-PBN administered just before recanalization reduced erythrocyte entrapment and ischemic lesion size, similarly to N-tert-butyl-α-phenylnitrone (PBN; **B**; scale bar=50 μm). S-PBN: N-tert-butyl-alpha-(2-sulfophenyl)nitrone. *P<0.05 vs saline-treated group, #P>0.05 vs S-PBN–treated group. Mice treated with S-PBN showed a significantly better and lasting outcome in corner turn and adhesive tape removal tests compared with the saline-treated group (**C** and **D**). *P=0.03. n=6 per group.

and differentially demonstrate suppression of ROS in parenchymal and vascular cells. This approach unambiguously led the below conclusions that were previously inferred based on relatively indirect observations and measurements:

1. PBN penetrates well to brain parenchyma and rapidly scavenges the oxygen radicals generated in parenchymal cells contrary to claims that PBN being a weak antioxidant does not reach to high-enough concentrations in the target tissue to be effective.[23] PBN also suppresses radicals generated in the vascular wall. Importantly, these observations exclude the possibility that the radicals generated within the vascular wall may consume PBN before reaching to parenchyma, suggesting that the dose of PBN used may provide protection by vascular and parenchymal actions in the mouse brain. These findings illustrate the potential of our model to choose the correct dose and dosing interval of an agent for the targeted pharmacological aims by directly observing them. The reduction in infarct volume does not necessarily indicate that the drug reached the parenchyma because these changes could be secondary to vascular protection. Differentiating between the parenchymal and vascular actions is required for gaining mechanistic insight and rationale drug development although determining the infarct size alone might seemingly be satisfactory as a clinically relevant end point in final analysis.
2. S-PBN does not penetrate parenchyma but effectively suppresses ROS generated within the vascular wall.

Interestingly, S-PBN also provides neuroprotection probably secondary to improved microcirculation after recanalization, which may then decrease ROS generation by parenchymal cells. Because S-PBN is lipophobic, it is not expected to penetrate brain parenchyma at this early time point after ischemia when tight junctions between the endothelia (the conduit for water-soluble molecules) are still intact.[28] Indeed, no measurable S-PBN was detected in the brain when administered to rats 3 hours after brain trauma although trauma rapidly causes BBB opening.[16] Furthermore, being a polar, lipophobic molecule, S-PBN is not expected to penetrate not only BBB but also into cells; hence, it is considered as an extracellular antioxidant.[29] Therefore, the reduction in ROS signal within parenchymal cells cannot be attributed to delayed penetrance of S-PBN through a leaky BBB but to improved microcirculation, which reduces the cellular metabolic stress to parenchymal cells and their radical generation. The latter argument is supported by demonstration of an intact BBB at the end of 1-hour i/r and improved rCBF after recanalization by laser speckle recordings.[31,32] This was further confirmed by showing prevention of erythrocyte entrapments within microcirculation by S-PBN. These observations verify that radical scavenging can prevent microvascular clogging after recanalization (no-reflow), as proposed previously.[8] However, unlike previous studies, here, we limited the duration of ischemia and recanalization to 1 hour and,

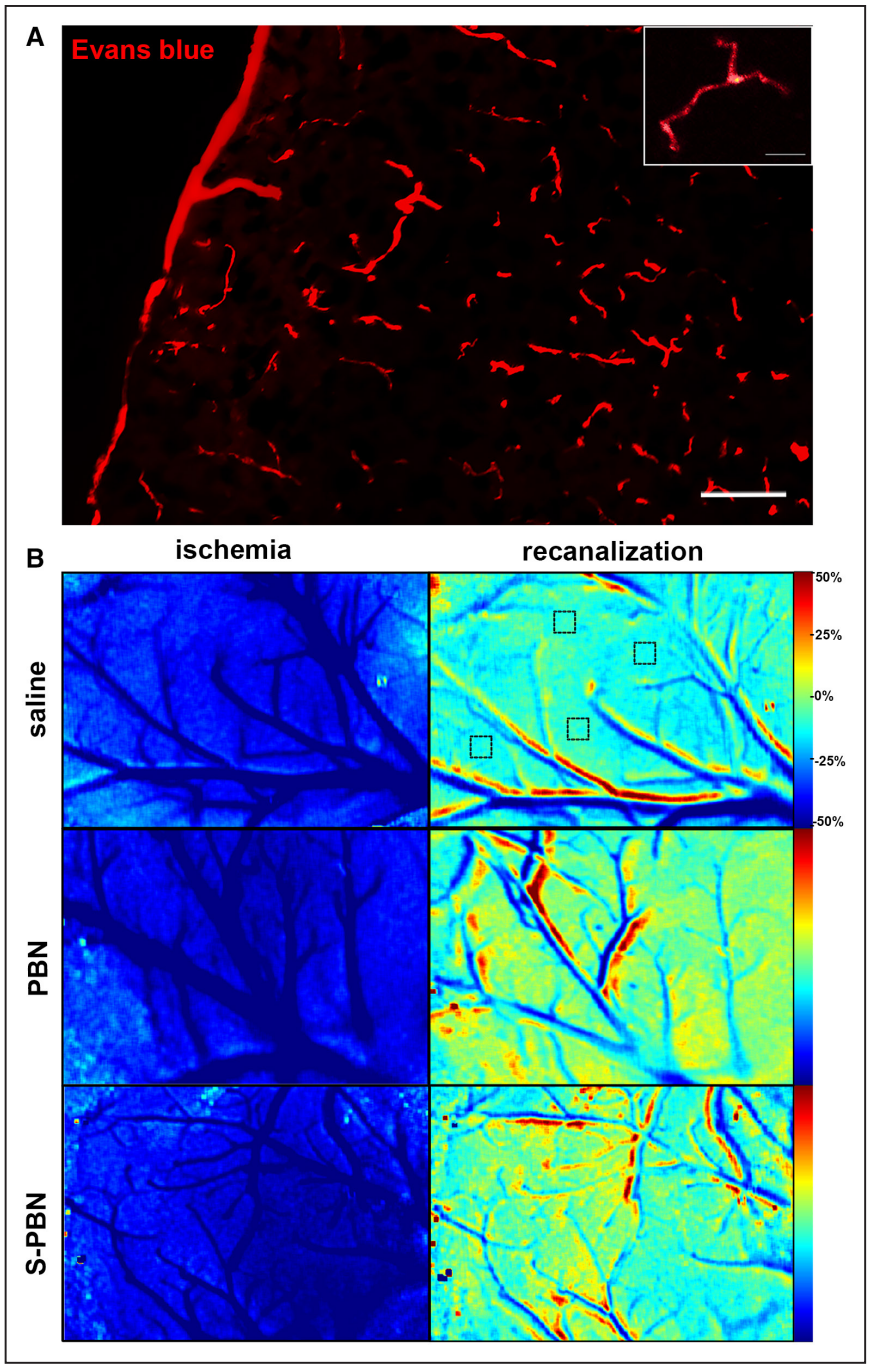

Figure 5. Blood–brain barrier (BBB) was still intact when 2-sulfo-phenyl-N-tert-butylnitrone (S-PBN) was administered. Systemically administered Evans blue did not leak into the tissue indicating that BBB was intact at the end of 1-hour ischemia/recanalization (**A**, a representative tile scan image of ischemic cortex acquired by laser-scanning confocal microscope; scale bar=100 μm; in inset, 10 μm). N-tert-butyl-α-phenylnitrone (PBN) improved tissue reperfusion after recanalization; representative mean rCBF-change maps acquired by laser speckle contrast imaging throughout ischemia and recanalization are illustrated for each group (**B**). Drift in *z* axis (vessel shift) was inevitable because of the blood volume changes in the ischemic/reperfused tissue. Scale bar on the right shows that cold colors represent a decrease, whereas hot colors, an increase in rCBF from baseline. The average values measured at 4 regions of interest (boxes) are given in the Table.

investigated all parameters at the end of 1-hour ischemia and 1-hour recanalization to minimize the effect of confounding factors that will develop during the course of ischemia. For example, later, PBNs may also act on inflammation, invasion of inflammatory cells, and opening of the BBB (eg, S-PBN action would not be limited to vasculature), all of which may modify the interpretation of our observations.[22,23]

These findings have important translational potential because evidence from recent clinical trials shows that recanalization does not always lead to reperfusion of the ischemic tissue in patients treated with tPA (tissue-type plasminogen activator) or interventional methods.[6,33] A recent study that specifically evaluated the relationship between reperfusion and recanalization reported that reperfusion could not be attained in 57% of the recanalized patients receiving tPA within 4.5 hours.[34] The incomplete reperfusion is not limited to intravenous tPA treatment but is also seen after intra-arterial recanalization therapies.[35] Experimental studies suggest that the damage induced by ischemia to microvessels limits reperfusion (no-reflow) after recanalization and plays a critical role in determining tissue survival.[5,8] Magnetic resonance studies specifically measuring capillary transit time in patients with stroke support these experimental findings and underscore the importance of capillary transit time heterogeneity in oxygenation of the ischemic tissue beyond the patency of upstream vessels.[36] In light of these recent developments, we think that therapies targeting microcirculation is the

next step to improve the success of recanalization therapies for ischemic stroke.[4] Combination of parenchymal protection with improving microvascular reperfusion is likely to be the ideal approach. Recent interventional trials clearly show that a prolonged therapeutic window exists if the tissue is supported by residual blood flow at penumbral levels, which creates hopes that tissue areas with lower flow levels can also be rescued by combining microvascular and parenchymal protection. Therefore, differential (parenchymal versus vascular) examination of the pharmacological end points targeted with radical scavengers or other antioxidant treatments in situ in intact animals may be highly instrumental in identifying the correct agents, dose, and dosing time to prevent clinical failures as experienced with NXY.[1] For example, neuroprotection observed with S-PBN administered 2 hours after MCA ischemia was hypothesized to be provided by penetration of S-PBN through damaged BBB[11] contrary to our findings in the present study. In the above study, the additional doses of S-PBN given after the first day are likely to have acted on inflammatory mechanisms because neurons are irreversibly damaged by 24 hours although the BBB becomes permeable to S-PBN. Similarly, detection of PBN or S-PBN levels in the brain after systemic administration cannot give a direct estimate of how efficiently radicals in different compartments were suppressed as demonstrated in our study. The method we developed in the present study is specifically tailored to investigate the postulated actions of antioxidant treatments to better predict their translational potential.

Acknowledgments

We thank Gökhan Uruk and Utku Norman for their technical assistance in MATLAB (Mathworks) calculations.

Sources of Funding

This study was supported by Hacettepe University, Scientific Research Projects Coordination Unit (011D04105001). Dr Dalkara's research is supported by the Turkish Academy of Sciences.

Disclosures

None.

References

1. Shuaib A, Lees KR, Lyden P, Grotta J, Davalos A, Davis SM, et al; SAINT II Trial Investigators. NXY-059 for the treatment of acute ischemic stroke. *N Engl J Med*. 2007;357:562–571. doi: 10.1056/NEJMoa070240.
2. Minnerup J, Sutherland BA, Buchan AM, Kleinschnitz C. Neuroprotection for stroke: current status and future perspectives. *Int J Mol Sci*. 2012;13:11753–11772. doi: 10.3390/ijms130911753.
3. Neuhaus AA, Couch Y, Hadley G, Buchan AM. Neuroprotection in stroke: the importance of collaboration and reproducibility. *Brain*. 2017;140:2079–2092. doi: 10.1093/brain/awx126.
4. Gursoy-Ozdemir Y, Yemisci M, Dalkara T. Microvascular protection is essential for successful neuroprotection in stroke. *J Neurochem*. 2012;123(suppl 2):2–11. doi: 10.1111/j.1471-4159.2012.07938.x.
5. Dalkara T, Arsava EM. Can restoring incomplete microcirculatory reperfusion improve stroke outcome after thrombolysis? *J Cereb Blood Flow Metab*. 2012;32:2091–2099. doi: 10.1038/jcbfm.2012.139.
6. Catanese L, Tarsia J, Fisher M. Acute ischemic stroke therapy overview. *Circ Res*. 2017;120:541–558. doi: 10.1161/CIRCRESAHA.116.309278.
7. del Zoppo GJ, Mabuchi T. Cerebral microvessel responses to focal ischemia. *J Cereb Blood Flow Metab*. 2003;23:879–894. doi: 10.1097/01.WCB.0000078322.96027.78.
8. Yemisci M, Gursoy-Ozdemir Y, Vural A, Can A, Topalkara K, Dalkara T. Pericyte contraction induced by oxidative-nitrative stress impairs capillary reflow despite successful opening of an occluded cerebral artery. *Nat Med*. 2009;15:1031–1037. doi: 10.1038/nm.2022.
9. Gaudin A, Yemisci M, Eroglu H, Lepetre-Mouelhi S, Turkoglu OF, Dönmez-Demir B, et al. Squalenoyl adenosine nanoparticles provide neuroprotection after stroke and spinal cord injury. *Nat Nanotechnol*. 2014;9:1054–1062. doi: 10.1038/nnano.2014.274.
10. Leger PL, Bonnin P, Moretti R, Tanaka S, Duranteau J, Renolleau S, et al. Early recruitment of cerebral microcirculation by neuronal nitric oxide synthase inhibition in a juvenile ischemic rat model. *Cerebrovasc Dis*. 2016;41:40–49. doi: 10.1159/000441663.
11. Yang Y, Li Q, Shuaib A. Neuroprotection by 2-h postischemia administration of two free radical scavengers, alpha-phenyl-n-tert-butyl-nitrone (PBN) and N-tert-butyl-(2-sulfophenyl)-nitrone (S-PBN), in rats subjected to focal embolic cerebral ischemia. *Exp Neurol*. 2000;163:39–45. doi: 10.1006/exnr.2000.7364.
12. Feuerstein GZ, Zaleska MM, Krams M, Wang X, Day M, Rutkowski JL, et al. Missing steps in the STAIR case: a translational medicine perspective on the development of NXY-059 for treatment of acute ischemic stroke. *J Cereb Blood Flow Metab*. 2008;28:217–219. doi: 10.1038/sj.jcbfm.9600516.
13. Arsava EM, Gurer G, Gursoy-Ozdemir Y, Karatas H, Dalkara T. A new model of transient focal cerebral ischemia for inducing selective neuronal necrosis. *Brain Res Bull*. 2009;78:226–231. doi: 10.1016/j.brainresbull.2008.11.005.
14. Dunn AK, Bolay H, Moskowitz MA, Boas DA. Dynamic imaging of cerebral blood flow using laser speckle. *J Cereb Blood Flow Metab*. 2001;21:195–201. doi: 10.1097/00004647-200103000-00002.
15. Zhao H, Joseph J, Fales HM, Sokoloski EA, Levine RL, Vasquez-Vivar J, et al. Detection and characterization of the product of hydroethidine and intracellular superoxide by HPLC and limitations of fluorescence. *Proc Natl Acad Sci USA*. 2005;102:5727–5732. doi: 10.1073/pnas.0501719102.
16. Marklund N, Lewander T, Clausen F, Hillered L. Effects of the nitrone radical scavengers PBN and S-PBN on in vivo trapping of reactive oxygen species after traumatic brain injury in rats. *J Cereb Blood Flow Metab*. 2001;21:1259–1267. doi: 10.1097/00004647-200111000-00002.
17. Chen GM, Bray TM, Janzen EG, McCay PB. Excretion, metabolism and tissue distribution of a spin trapping agent, alpha-phenyl-N-tert-butylnitrone (PBN) in rats. *Free Radic Res Commun*. 1990;9:317–323.
18. Liu S, Connor J, Peterson S, Shuttleworth CW, Liu KJ. Direct visualization of trapped erythrocytes in rat brain after focal ischemia and reperfusion. *J Cereb Blood Flow Metab*. 2002;22:1222–1230. doi: 10.1097/01.wcb.0000037998.34930.83.
19. Ayata C, Dunn AK, Gursoy-Ozdemir Y, Huang Z, Boas DA, Moskowitz MA. Laser speckle flowmetry for the study of cerebrovascular physiology in normal and ischemic mouse cortex. *J Cereb Blood Flow Metab*. 2004;24:744–755. doi: 10.1097/01.WCB.0000122745.72175.D5.
20. Karatas H, Erdener SE, Gursoy-Ozdemir Y, Gurer G, Soylemezoglu F, Dunn AK, et al. Thrombotic distal middle cerebral artery occlusion produced by topical FeCl(3) application: a novel model suitable for intravital microscopy and thrombolysis studies. *J Cereb Blood Flow Metab*. 2011;31:1452–1460. doi: 10.1038/jcbfm.2011.8.
21. Davis MA, Gagnon L, Boas DA, Dunn AK. Sensitivity of laser speckle contrast imaging to flow perturbations in the cortex. *Biomed Opt Express*. 2016;7:759–775. doi: 10.1364/BOE.7.000759.
22. Green AR, Ashwood T, Odergren T, Jackson DM. Nitrones as neuroprotective agents in cerebral ischemia, with particular reference to NXY-059. *Pharmacol Ther*. 2003;100:195–214.
23. Floyd RA, Kopke RD, Choi CH, Foster SB, Doblas S, Towner RA. Nitrones as therapeutics. *Free Radic Biol Med*. 2008;45:1361–1374. doi: 10.1016/j.freeradbiomed.2008.08.017.
24. Kuroda S, Tsuchidate R, Smith ML, Maples KR, Siesjö BK. Neuroprotective effects of a novel nitrone, NXY-059, after transient focal cerebral ischemia in the rat. *J Cereb Blood Flow Metab*. 1999;19:778–787. doi: 10.1097/00004647-199907000-00008.
25. Cao X, Phillis JW. Alpha-Phenyl-tert-butyl-nitrone reduces cortical infarct and edema in rats subjected to focal ischemia. *Brain Res*. 1994;644:267–272.
26. Morancho A, García-Bonilla L, Barceló V, Giralt D, Campos-Martorell M, Garcia S, et al. A new method for focal transient cerebral ischaemia by distal compression of the middle cerebral artery. *Neuropathol Appl Neurobiol*. 2012;38:617–627. doi: 10.1111/j.1365-2990.2012.01252.x.

27. Bouet V, Boulouard M, Toutain J, Divoux D, Bernaudin M, Schumann-Bard P, et al. The adhesive removal test: a sensitive method to assess sensorimotor deficits in mice. *Nat Protoc*. 2009;4:1560–1564. doi: 10.1038/nprot.2009.125.
28. Knowland D, Arac A, Sekiguchi KJ, Hsu M, Lutz SE, Perrino J, et al. Stepwise recruitment of transcellular and paracellular pathways underlies blood-brain barrier breakdown in stroke. *Neuron*. 2014;82:603–617. doi: 10.1016/j.neuron.2014.03.003.
29. Hobbs CE, Murphy MP, Smith RA, Oorschot DE. Neonatal rat hypoxia-ischemia: effect of the anti-oxidant mitoquinol, and S-PBN. *Pediatr Int*. 2008;50:481–488. doi: 10.1111/j.1442-200X.2008.02705.x.
30. Wang Y, Yamamoto S, Miyakawa A, Sakurai T, Ibaraki K, Terakawa S. Intravital oxygen radical imaging in normal and ischemic rat cortex. *Neurosurgery*. 2010;67:118–127; discussion 127. doi: 10.1227/01.NEU.0000370055.99998.6B.
31. Wang Z, Hughes S, Dayasundara S, Menon RS. Theoretical and experimental optimization of laser speckle contrast imaging for high specificity to brain microcirculation. *J Cereb Blood Flow Metab*. 2007;27:258–269. doi: 10.1038/sj.jcbfm.9600357.
32. Kazmi SM, Richards LM, Schrandt CJ, Davis MA, Dunn AK. Expanding applications, accuracy, and interpretation of laser speckle contrast imaging of cerebral blood flow. *J Cereb Blood Flow Metab*. 2015;35:1076–1084. doi: 10.1038/jcbfm.2015.84.
33. Khandelwal P, Yavagal DR, Sacco RL. Acute ischemic stroke intervention. *J Am Coll Cardiol*. 2016;67:2631–2644. doi: 10.1016/j.jacc.2016.03.555.
34. Horsch AD, Dankbaar JW, Niesten JM, van Seeters T, van der Schaaf IC, van der Graaf Y, et al; Dutch Acute Stroke Study Investigators. Predictors of reperfusion in patients with acute ischemic stroke. *AJNR Am J Neuroradiol*. 2015;36:1056–1062. doi: 10.3174/ajnr.A4283.
35. Al-Ali F, Jefferson A, Barrow T, Cree T, Louis S, Luke K, et al. The capillary index score: rethinking the acute ischemic stroke treatment algorithm. Results from the borgess medical center acute ischemic stroke registry. *J Neurointerv Surg*. 2013;5:139–143. doi: 10.1136/neurintsurg-2011-010146.
36. Mouridsen K, Hansen MB, Østergaard L, Jespersen SN. Reliable estimation of capillary transit time distributions using DSC-MRI. *J Cereb Blood Flow Metab*. 2014;34:1511–1521. doi: 10.1038/jcbfm.2014.111.